Impact of arginine modified SNARE peptides on interactions with phospholipid bilayers and coiled-coil formation: A molecular dynamics study

Journal of Molecular Liquids 364 (2022) 119972

Contents lists available at ScienceDirect

Journal of Molecular Liquids

journal homepage: www.elsevier.com/locate/molliq

Impact of arginine modified SNARE peptides on interactions with phospholipid bilayers and coiled-coil formation: A molecular dynamics study

Bence Fehér *, Levena Gascoigne, Sanne N. Giezen, Ilja K. Voets *

Laboratory of Self-Organizing Soft Matter, Department of Chemical Engineering and Chemistry, Eindhoven University of Technology, P.O. Box 513, 5600 MB Eindhoven, the Netherlands

ARTICLE INFO

Article history:
Received 30 April 2022
Revised 25 July 2022
Accepted 27 July 2022
Available online 4 August 2022

Keywords:
SNARE
Membrane
Fusion
Arginine
Molecular dynamics

ABSTRACT

Membrane fusion plays a vital role in several biological processes such as cellular uptake, communication between cells and RNA delivery. Due to its complexity, model membranes and minimalistic fusion protein models are often used to gain insight into the fusion process. Coiled–coil (CC) peptides, consisting of two to five α–helical peptides, are highly advantageous as minimalistic protein models. One of the most common fusion CC complex is formed between the complementary peptides E ($(KIAALKE)_4$) and K ($(EIAALEK)_4$). In this system, K peptides have been suggested to prime the membrane for fusion by causing small lipid protrusions within the membrane, increasing local curvature and membrane dehydration. In this study, we develop a library of peptides based on K peptide sequence by substituting lysine amino acids with arginine at varying heptad locations. By molecular dynamics simulations, we find that increasing the amount of arginine in the peptides results in enhanced affinity to the membrane. With coarse-grained simulations, we show that the interaction of peptides with the membrane triggers increased curvature in the membrane without significantly disrupting the lipid packing. Additionally, we find that all modified peptides retain the capability of forming CC complexes with E peptides. Our results suggest that arginine positioning is critical when designing CC fusion peptides. Peptides with arginines located at the N–terminus (ARG1, ARG6) show greater affinity to the lipid membrane. Our simulations suggest that introducing arginine into CC peptide sequences can enhance the binding affinity to the membrane via hydrogen bonds and may lead to more effective CC fusion peptides than E–K complexes.

1. Introduction

Fusion between lipid membranes is a fundamental process in many biological events such as viral infection, fertilization, and the delivery of impermeable molecules [1,2]. In order to promote fusion, opposing membranes must overcome electrostatic, hydration and steric barriers. Once docked, the membranes undergo extreme shape transformations and form non-bilayer intermediates. Eventually, lipid molecules will re-arrange to form a lipid stalk and undergo outer lipid mixing. Finally, an aqueous fusion pore is formed, and content between cells is shared (see Fig. 1A for fusion details). In cells, this highly complex process is aided by fusion proteins (fusogens). Due to the complexity of biological membranes and fusogens, elucidating the role of individual components involved in fusion is difficult, and exact mechanisms remain unknown. Therefore, model membranes and model fusogens are often employed to gain fundamental knowledge on the minimal requirements for membranes to fuse. Membrane models are normally small and large liposomes composed of 1,2-dio leoyl-sn-glycero-3-phosphocholine (DOPC), 2-dioleoyl-sn-gly cero-3-phosphoethanolamine (DOPE) and cholesterol (50/25/25 mol%). DOPE is often incorporated into the membrane specifically to enhance the rate of fusion and formation of stalk intermediate due to the highly negative curvature nature of the lipid [3–5]. One of the most promising minimalistic fusogen model systems is based on the coiled-coil (CC) complex of soluble N-ethylmaleimide-sensitive factor attachment protein receptors (SNARE). CC peptide structures have been intensely investigated out of fundamental and applied interest in supramolecular assembly, biosensing, liposomal fusion and super-resolution microscopy [6–9]. CCs are less complex in their secondary structure compared to large proteins, but remain highly diverse in their function. This decrease in structural complexity makes designing small functional proteins easier [10–12] The secondary structure of CCs can consist of two to five α-helical peptides that twist around each

* Corresponding authors.
E-mail addresses: b.feher@tue.nl (B. Fehér), I.Voets@tue.nl (I.K. Voets).

https://doi.org/10.1016/j.molliq.2022.119972
0167-7322/

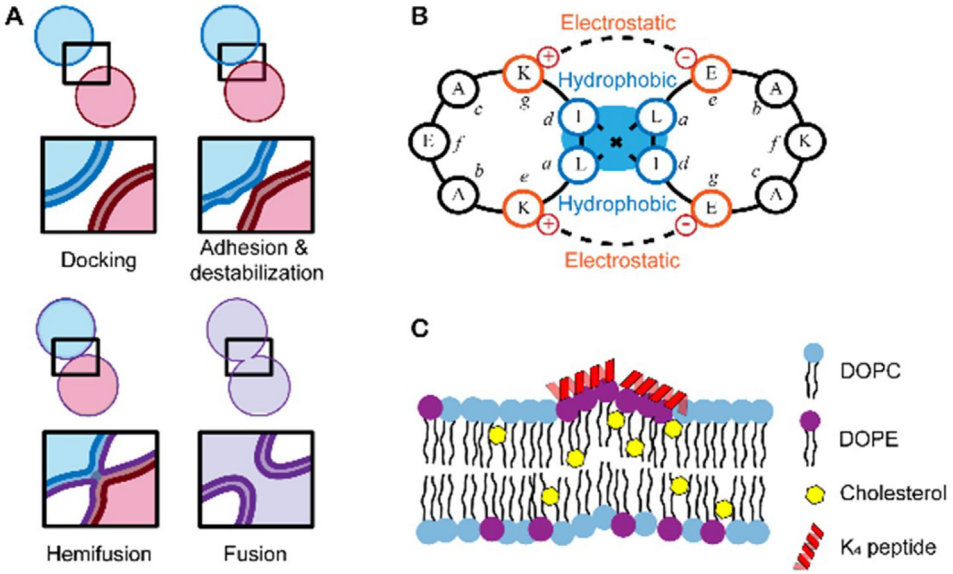

Fig. 1. A: Scheme of fusion mechanism, B: E–K coiled-coil complex helical wheel diagram. The driving forces for the formation of a coiled-coil complex are the attractive interactions between the hydrophobic residues at *a* and *d* and oppositely charged residues on *g* and *e* and C: membrane disruption by K_4.

other, forming a left-handed supercoil. Typically, CCs are constructed of heptad repeating hydrophobic and polar residues, denoted by *a, b, c, d, e, f, g* (Fig. 1B) [13]. One of the main driving forces for creating a CC complex is the hydrophobic effect. Hydrophobic amino acids (typically leucine and isoleucine) located at positions *a* and *d*, will pack to minizine their interaction with surrounding water molecules to form a hydrophobic core [14]. The association strength and stability of CCs are also affected by the presence of charged amino residues at *e* and *g* locations [14]. Often, oppositely charged residues stabilize inter-helical formation due to electrostatic attraction, whereas opposing peptides with like charges will lead to destabilization due to electrostatic repulsion [14]. Locations *e* and *g* act as specific trigger sights for the formation of CC, having distinctive intra— and intermolecular forces such as ionic attraction and hydrogen bonding [15–18]. Tuning these critical parameters during peptide design allows to create CC complexes tailored for specific applications.

CC designs targeting fusion are often based on simplified SNARE proteins. One of the most common complex is formed between the complementary peptides E (KIAALKE) and K (EIAALEK). Typically, repeating units of (K_n) and (E_n) are conjugated to a cholesterol membrane anchor, which is tethered to a polyethylene glycol (PEG) linker [8,19,20]. For the occurrence of E–K mediated fusion, strong binding interactions between E and K membrane-tethered peptides are required to dock opposing membranes together [21]. Additionally, the K peptide has been suggested to prime the membrane for fusion by causing small lipid protrusions within the membrane. All-atomistic and coarse-grained molecular dynamics simulations of the interaction of E and K peptides with lipid membranes have shown that only K interacts with the membrane. This causes an increase in local curvature and distortion of the membrane [22–24], which primes the membrane for fusion [25,26] Mechanistically, the adsorbed peptide causes increased curvature via the accumulation of DOPE and cholesterol around the absorbed K peptide (Fig. 1C), while membrane distortions are thought to originate from the displacement of water molecules from the lipid hydration layer.

The impact on fusion of numerous modifications to the E–K fusion system have been investigated, such as PEG linker length, [27] lipid anchor composition,[28] and the number of heptad repeats [20]. More recently, variations to the hydrophobic core (altering type of amino acid residues *a* and *d*) have been conducted [8]. These studies primarily aim to achieve increase in CC strength to augment fusion efficiency. Underexplored is the impact of enhanced affinity of the K peptide for the membrane to promote its adsorption. We propose that the number of dehydrating amino acids within the K yields enhanced affinity of peptide to the membrane, enhancing the promotion of fusion. To evaluate this conjecture, we substituted lysine amino acids at locations *e* and *g* by arginine. Arginine has same charge as lysine, and carries a guanidium instead of an amine functionality in its side chain. Interestingly, this allows to enhance peptide–membrane interactions through strong guanidium–phosphate bonds[29–31] without compromising the electrostatic interactions with glutamic acid, which are essential for CC formation [30].

In this work we will apply all-atomistic and coarse-grained molecular dynamics simulations to evaluate the capability of arginine modified peptides to interact with phospholipid membrane. Furthermore, we will explore whether arginine incorporation impacts the ability of the peptides to form α-helices and CC complexes with the opposing E peptide. Lastly, we assess whether arginine modified peptides' bind preferentially to either lipid membrane or E partner peptides.

2. Methods

All-atomistic and coarse-grained molecular dynamics simulation was performed with Gromacs 2019.6 [32,33], on membrane, peptide–membrane, peptide–peptide and peptide–peptide–membrane systems. For all-atomistic simulations, a membrane composed of 42 1,2-dioleoyl-sn-glycero-3-phosphoethanolamine (DOPE), 82 1,2-dioleoyl-sn-glycero-3-phosphocholine DOPC and 42 cholesterol was chosen, while for coarse-grained simulation 294, 588 and 294 lipids molecules were involved, respectively. The lipid ratios in the upper and lower leaflets are both 1:2:1 for DOPE:DOPC:cholesterol. The peptide–membrane simulations were set up with the same membrane composition with the addition of 5 different peptide sequences (Table 1). The system was solvated in a cubic box with TIP3P water model and neutralized with Na^+ and Cl^- ions. 3 independent simulations were performed for each sys-

Table 1
Sequence of arginine modified SNARE peptides.

Name	Sequence $(gabcdef)_4$	Electrostatic pattern
E_4	EIAALEK EIAALEK EIAALEK EIAALEK	E E E E
K_4	KIAALKE KIAALKE KIAALKE KIAALKE	K K K K
R_4	RIAALRE RIAALRE RIAALRE RIAALRE	R R R R
$R_{1.1}$	RIAALRE KIAALKE KIAALKE KIAALKE	R K K K
$R_{1.4}$	KIAALKE KIAALKE KIAALKE RIAALRE	K K K R

tem with different initial coordinates of the peptide. Peptide conformations were predicted in PEPFold 3 [34–36]. The initial coordinates were constructed and initially equilibrated using CHARMM-GUI membrane builder [37,38]. The input of the peptide–peptide–membrane systems were constructed from the output of the appropriate peptide–membrane simulation with the addition of the second peptide. The simulation protocol was the same after the insertion of the second peptide as for the previous systems. All-atomistic simulations were performed using CHARMM36 [39,40] force field. Our systems were minimized for 5000 steps using the steepest descent method. Subsequently, the systems were equilibrated for 750 ps at constant temperature of 303.15 K and 1 bar with integration time step of 2 fs. The particle–mesh Ewald (PME) method was applied to calculate the long-range electrostatic interactions [41,42] with 1.2 nm cutoff distance. Van der Waals interactions were treated with a cutoff of 1.2 nm. The temperature was kept stable using the Nose–Hoover thermostat [43–45] with 1 ps coupling time. The pressure was controlled semi-isotropically by a Parrinello-Rahman barostate [46] with 5 ps coupling time. Hydrogens were constrained by LINCS algorithm [47]. The simulation time was 100 ns.

For simulation of peptide–peptide interaction R_4, $R_{1.1}$ or $R_{1.4}$ with E_4 were inserted in a cubic box with 3 nm distance from the box edges. 50 or 75 ns simulation was performed with the same parameters as for peptide–membrane simulations (except that the pressure was controlled isotropically).

Coarse-grained simulations were performed using Martini 2.2p force field [48] with polarizable water model [49]. The relative permittivity of the medium was 2.5. The systems was neutralized with Na^+ and Cl^- ions. Our systems were minimized for 5000 steps using the steepest descent method, followed by 1000 ps equilibration with integration time step of 2 fs. PME method was applied to calculate the long-range electrostatic interactions with 1.1 nm cutoff distance. Van der Waals interactions were treated with a cutoff of 1.1 nm. The temperature was kept constant with velocity rescale thermostat [50] with 1 ps coupling time, and the pressure was maintained by Parrinello-Rahman barostate with 12 ps coupling time. The simulation time was 300 ns. Visualization and hydrogen bond analysis was performed in Chimera 1.3 [51]. The mean average curvature was calculated with MDAnalysis MembraneCurvature Python toolkit [52,53].

3. Results and Discussion

3.1. Arginine substitutions enhance interactions with liposomal membranes

To assess the impact of various substitutions in the K peptide on its interaction with liposomal membranes, we investigated R_4, $R_{1.1}$ and $R_{1.4}$ peptides differing in composition (Table 1). Namely, R_4 consists of two arginine residues in each of the 4 heptads, whilst lysines are substituted by arginines in only one out of the four heptads in $R_{1.1}$ (1st heptad) and $R_{1.4}$ (4th heptad). The peptides were positioned in the vicinity of the lipid membrane, after which their

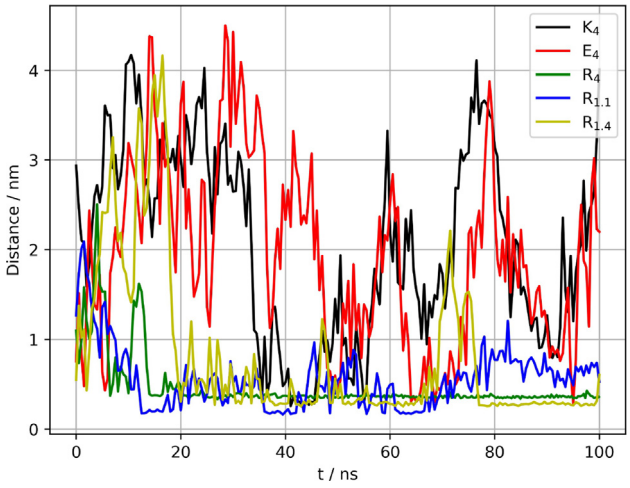

Fig. 2. Minimum distances of peptides from the surface of the membrane.

distance from the lipid headgroups (Fig. 2) was monitored for 100 ns. We performed the simulation at 303.15 K due to the fact that at higher temperatures the simulation converges faster than at room temperature and we presume that the slightly elevated temperature does not cause big difference in the interactions. Interestingly, the five peptides interact rather differently with the membrane. Snapshots of simulations at 0, 50 and 100 ns of each peptide are shown in the Supplementary (ESI Fig. S1). The relatively large distance between the E_4 peptide and the membrane throughout the 100 ns simulation suggests that E_4 does not have a strong affinity for the membrane. This is in line with coarse-grained simulations previously reported by others [25,26]. Surprisingly, K_4 does not appear to adsorb significantly onto the membrane either. This is in contrast with earlier reports on coarse-grained simulations [23,54], which revealed a stronger affinity of K_4 peptide for membranes. Tentatively, we propose that the interaction is too weak to induce significant binding during the limited runtime of the atomistic simulations. For practical reasons, we nonetheless maintained the short runtime and tested whether arginine substitutions led to detectable reduction in the relative distance between the peptide and membrane signalling enhanced interaction. According to our results all arginine-containing peptides (R_4, $R_{1.1}$ and $R_{1.4}$) resided in closer proximity to the membrane than either the K_4 or E_4 peptide, indicative of increased affinity. The interaction is most prominent for R_4. This peptide went in contact with the membrane after 20 ns and stayed in contact throughout the remainder of the simulation via the N–terminus of the arginine residue. $R_{1.1}$ behaves slightly differently. It approaches the surface approximately after 15 ns and binds via the N–terminus of arginine; however, its minimum distance fluctuates much more than R_4 (which is within 0.5 nm after 20 ns) but never exceeds 1 nm. In order to exclude any artefact originating from the initial position of the peptide, 3 independent simulations were performed with different orientations of the peptide, and all results show very similar trends. Interestingly, $R_{1.4}$ shows different behaviour than the other peptides. After 40 ns it becomes bound to the membrane, but some peaks arise, showing that the peptide moves away from the membrane, and then makes contact again. Despite the presence of the two relatively large peaks at 10 and 70 ns (minimum distance of approximately 1 and 2 nm), the $R_{1.4}$ is in closer contact with the membrane than $R_{1.1}$. These findings suggest that greater number of arginines in the peptide promotes peptide–membrane interactions. The membrane affinity appears largest for R_4, followed by $R_{1.1}$ and $R_{1.4}$.

3.2. Hydrogen bond analysis of membrane–peptide complexes

To complement the minimum distance analysis, which offers only qualitative impression of the affinity of the various peptides for the membrane and is too coarse to identify slight differences in affinity, we turned to hydrogen bond analysis. The number of hydrogen bonds between the peptides and lipid molecules was calculated throughout the whole trajectory (Fig. 3). The curves clearly show that for non-interacting peptides K_4 and E_4, the number of hydrogen bonds is either 0 or randomly fluctuates. However, in the case of R_4, it gradually increases up to 50 ns and fluctuates around 9 for the whole simulation. $R_{1.1}$ fluctuates in the first 60 ns then drops, followed by an increase again and fluctuates around 10 from 85 ns. $R_{1.4}$ shows more hydrogen bonds than K_4 and E_4, but less than R_4 and $R_{1.1}$. Furthermore, we calculated the hydrogen bond lifetimes for R peptides based on continuous hydrogen bond autocorrelation functions described by van der Spoel et al. [55] We calculated the values for the last 50 ns of the simulation. The values for all systems are collected in Table 3. The results show longer lifetime for R_4 than for $R_{1.1}$ and $R_{1.4}$, which are comparable. Note that the small relaxation time values are due to the application of continuous hydrogen bonds, which means that when a hydrogen bond breaks up and reforms it does not count as a single hydrogen bond. To elucidate which residues are responsible for the membrane binding with interacting peptides, we calculated the contribution of each residue to the total number of hydrogen bonds. As presented in Fig. 3B–D, B–D, arginine residues are responsible for almost all hydrogen bonds between the peptide and the membrane in all cases. The hydrogen bonds formed by the arginine between R_4, $R_{1.1}$ and $R_{1.4}$ display the same trend as the total hydrogen bond values seen in Fig. 3A. However, the incline of the curves are different. R_4 increases gradually until approximately 65 ns, while $R_{1.1}$ sharply increases from 10 ns. $R_{1.4}$ shows a peak at 80 ns and a slight decrease. The fluctuations of the values are due to hydrogen bonds being identified according to geometrical parameters; namely, the donor–acceptor distance must be less than 0.35 nm and the hydrogen–donor–acceptor angle must be smaller than 30° [56]. Since the peptide is dynamically moving and not a stiff molecule, the geometrical requirements are not always fulfilled, but the trend is apparent. The hydrogen bond analysis supports our conclusions based on the minimum distances. The above results suggest that arginine plays important role in membrane binding in two ways. Firstly, it appears that it is important that the N–terminus of the peptide be arginine (R_4 and $R_{1.1}$) and not lysine residue ($R_{1.4}$) to initiate peptide binding on the membrane. Secondly, the more arginines present in the sequence, the stronger membrane affinity the peptide will likely have.

3.3. Effect of membrane binding on peptide conformation

Membrane induced structural changes are common to many membrane interacting peptides. To reveal any conformational changes of membrane interacting peptides, we calculated the Ramachandran plot of the peptides (ESI Fig. S2). For R_4 it can be seen that the vast majority of the structure is right-handed α-helical, and only two residues close to the C–terminus adopted a different structure upon interaction with the membrane. In the case of $R_{1.1}$ the effects are similar. However, in the case of $R_{1.4}$, changes are more significant and both N– and C–terminus are affected. The core of $R_{1.4}$ peptide remains intact, however β-sheet-like and left-handed α-helical structural elements occur within the peptide. These results show that membrane binding does not influence significantly the secondary structure of the studied peptides.

3.4. Effect of interaction on lipid ordering

To gain insight into the changes in bilayer structure caused by the peptide, we calculated the lipid thickness throughout the

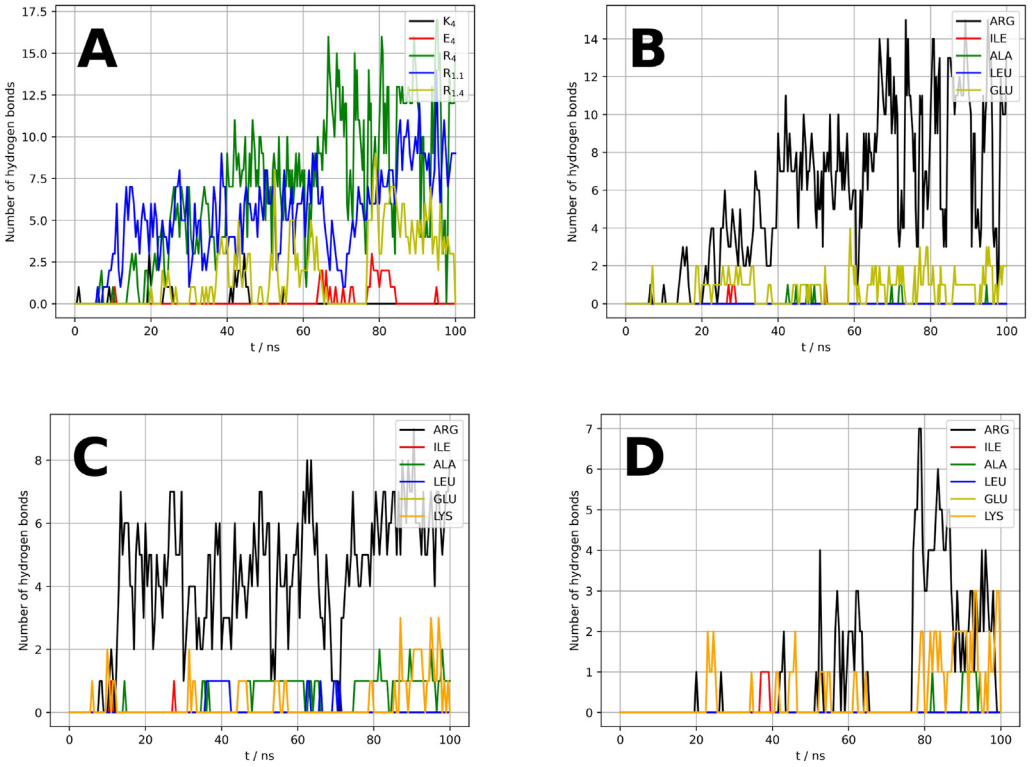

Fig. 3. Number of hydrogen bonds of A: peptides with lipid molecules, B: residues of R_4, C: residues of $R_{1.1}$ and D: residues of $R_{1.4}$ with lipids.

whole simulation. We also simulated a bilayer with the same composition without the peptide as a reference. In all simulations, the membrane thickness stays intact in the presence of the peptide at between 4.5 and 5 nm. To reveal any change to the ordering of lipids we calculated the deuterium order parameters (Scd) [57–60] for sn-1 and sn-2 chains of DOPE and DOPC separately. The Scd is the measure of the restriction of C–H bond vectors in the lipid tail, and it describes the ordering of hydrocarbon chains. Scd is defined by the orientation of all C–H bond vectors with respect to the bilayer normal and averaged over the lipids and over the time. Scd can be defined as

$$\mathrm{Scd} = \frac{\langle 3\cos^2\theta - 1\rangle}{2} \quad (1)$$

where θ is the angle between the C–H bond vector and bilayer normal, while the angular brackets stands for molecular and temporal ensemble average [59].

The Scd was calculated and averaged for the last 50 ns second of the simulation, where the interaction could be observed. Since we do not expect the peptide to change the lipids' ordering through the whole membrane, we split the lipid molecules into two groups. Those lipids within 1.5 nm cut-off distance from the peptide (any atoms of the two molecules are within 1.5 nm) are considered binding lipids. Those lipids out of the cut-off distance are considered non-binding lipids. The ordering of both DOPE and DOPC lipids close to the surrounding of R_4 appear to be affected by the peptide interaction (Fig. 4). In all cases, the change of Scd value of carbon 1 to 6 is more significant, which is closer to the headgroup, thus to the interaction site of the lipids. In the case of $R_{1.1}$, the change in Scd values are more significant, showing that the $R_{1.1}$ has a greater influence on lipid packing. The Scd values for $R_{1.4}$ resemble that of R_4; however, the changes are more significant in this case of DOPE for carbons 11–16. Our results suggest that even tough the lipid–peptide interaction does not affect the bilayer globally, it causes local fluctuation in the membrane close to the peptide. $R_{1.1}$ could be more membrane intrusive by snorkeling the arginine on the N–terminus into the lipid bilayer, while R_4 would not exhibit such snorkeling behaviour due to the spread of arginine moieties across the membrane. Thus, the peptide is more likely to remain parallel to the lipid membrane.

3.5. Effect of interaction on membrane curvature

The desired effect of SNARE peptides on phospholipid bilayers is the enhanced curvature to initiate membrane fusion; thus, it is essential to predict whether peptides influence membrane curvature. Coarse-grained molecular dynamics simulations are more suited to investigate membrane curvature than all-atomistic simulations since the curvature change is more pronounced in extended membranes, which requires much longer computational times. Consequently, we performed coarse-grained simulations of membrane–peptide systems, which are shown to have interactions by all-atomistic simulations. We performed the simulations in Martini force field, which uses a so-called 'four-to-one' mapping, which means that one bead replaces four heavy (not hydrogen) atoms. As a reference, we set up a simulation of the membrane without peptide with 294 DOPE, 588 DOPC and 294 cholesterol molecules and performed MD simulations for 300 ns. For the simulated systems, we calculated the mean average curvature (H) (Fig. 5). The mean membrane curvature of the membrane in the absence of peptides is homogeneous across the whole membrane; however, R_4 and R_{11} cause significant fluctuations in the membrane. $R_{1.4}$ only slightly affects the mean curvature. These results support our conclusions regarding binding affinity based on the all-atomistic simulations.

3.6. Probability of forming coiled–coil complex

For the designed peptides it is critical that they can form coiled-coil complex with the E peptide. Therefore, we investigated the probability of R_4, $R_{1.1}$ and $R_{1.4}$ forming CC complex with opposing E peptide and evaluated their intermolecular interactions. The simulation suggested attractive interaction between peptides in all cases (Fig. 6B, C, D). The hydrogen bond analysis of the whole trajectory shows that all of the R peptides form hydrogen bond with E_4 in slightly different extent. Hydrogen bond lifetimes (Table 3) shows that $R_{1.4}$ forms more stable hydrogen bonds with E_4 than R_4 and $R_{1.1}$. At the end of the simulations, hydrogen bonds were detected with the same geometrical parameters as above (Table 2). Similarly to K_4, R_4 forms the expected parallel CC complex. The analysis shows that arginine residues of R_4 forms hydrogen bonds with the glutamine, alanine and leucine of E_4. It is also apparent from the snapshots that R_4 (dark blue) undergoes reasonable conformational change close to C–terminus upon complexation. Similarly, with peptide–membrane interaction, for more precise analysis of the conformational transition, the Ramachandran plot was calculated (ESI Fig. S3). It shows that R_4 residues 21–26 (GLU21, ARG22, ILE23, ALA24, ALA25, LEU26) transform from α-helical to probably right-twisted β-sheets. Whereas $R_{1.1}$, does form parallel CC complex with no significant changes to α-helix structures. However, there is a shift in expected CC conformation and the N–terminus of $R_{1.1}$ is located midway of the E peptide. As it is suggested by the Ramachandran plot (ESI Fig. S3) $R_{1.1}$ undergoes conformational change approximately at the same extent as R_4 but the E_4 conformational transformation is more pronounced both close to N– and C–terminus. In this case to obtain stable structure, 70 ns simulation was necessary. Finally, between $R_{1.4}$ and E_4, the lysine residues are responsible for the hydrogen bonds, while glutamic acid, alanine and lysine take part in the interaction from E_4 side. The conformational change of peptides is not significant (ESI Fig. S3). In that case, the peptides in the CC are more parallel than $R_{1.1}$ and E_4 form complex more resembling R_4–E_4 structure.

We conclude that the multiple binding capability of arginine results in a competition between the two binding sites, while the hydrogen bond formed with the participation of lysine (which can form only one hydrogen bond) is more intact. Consequently, the incorporation of arginine into our peptide sequences may increase peptide–membrane interactions but could decrease CC formation.

3.7. Probability of forming coiled–coil complex on the membrane

As final evaluation for arginine modified peptides to be useful as fusogens, we investigated the affinity for the modified peptides to form CC complex also when bound to the membrane. We started the simulations from the last frame of R_4, $R_{1.1}$ and $R_{1.4}$ from our peptide–membrane simulation and inserted E_4 (red) randomly into the box (ESI Fig. S4). At the beginning of the simulation the E_4 moves randomly in the simulation box for each run. By 50 ns E_4 interacts with R_4 and remains close the R_4 which is bonded to the membrane. R_4 stays in the membrane surface throughout the whole simulation. In the case of $R_{1.1}$ the E_4 moves independently of $R_{1.1}$–membrane complex, however by the end of the 100 ns it also interacts with $R_{1.1}$ which remains on the surface. In the $R_{1.4}$–E_4–membrane system, $R_{1.4}$ is not completely stuck to the surface, moves more independently and does not appear to form CC complex.

To get deeper insight to the affinity of the arginine variations to the membrane surface and to E_4 we performed hydrogen bond analysis (Fig. 7). As it can be seen in Fig. 7A R_4 forms significantly more hydrogen bonds with the membrane than with E_4. Furthermore the number of hydrogen bonds between R_4 and the mem-

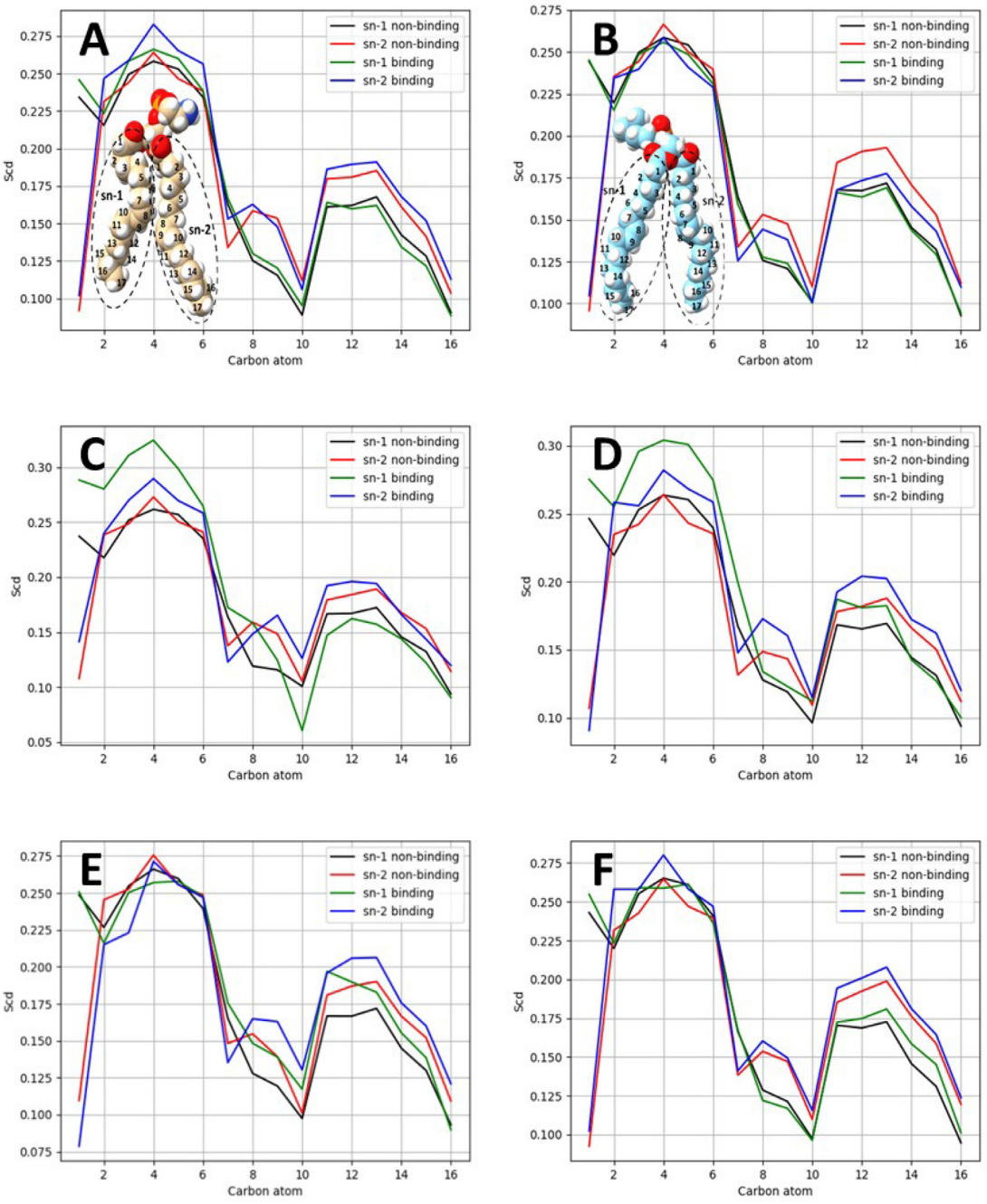

Fig. 4. Deuterium order parameter (Scd) of (A, C, E): DOPE and (B, D, F): DOPC acyl chains in the presence of (A, B): R_4, (C, D): $R_{1.1}$ and (E, F): $R_{1.4}$.

brane remains a large number. Between E_4 and the membrane there is no observed hydrogen bonds. In the case of E_4–$R_{1.1}$–membrane system (Fig. 7B) similar trends can be observed, however the number of hydrogen bonds between $R_{1.1}$ and the membrane significantly decreases. In the case of E_4–$R_{1.4}$–membrane system (Fig. 7C) significant affinity of the peptide to the membrane cannot be observed which is in agreement with our previous findings. Hydrogen bond lifetimes (Table 3) show the same trends.

We also performed hydrogen bond analysis on the last frame to identify the residues responsible for the interaction. Our results show that R_4 forms hydrogen bond with the membrane surface via residues ARG1, ILE2, ALA3, ARG6, ARG8 and ARG15. It appears that the N–terminus has greater affinity with lipid membrane, and this allows R_4 to form hydrogen bonds at residues ARG13 and ARG27 with E_4 at GLU6 and GLU20 residues. After binding to E_4, slight changes to R_4–membrane occur where R_4 forms hydrogen bond with the membrane surface via ARG1, LEU5, ARG6, ARG8 and ARG25. This shows that the preformed hydrogen bonds between R_4 and the membrane surface are not broken by the interaction with E_4, but it forms hydrogen bond with arginines of R_4 which are not involved in surface binding. For $R_{1.1}$, ARG1, ALA4 and ARG6 forms hydrogen bond with the membrane before the interaction with E_4. After the simulation ARG1 and LEU5 from R_4 forms hydrogen bond with the membrane, and LYS13 and LYS20 from R_4 interact with the GLU20 and GLU15 residues of E_4, respectively. This shows that the E_4 does not remove $R_{1.1}$ completely from the membrane, however $R_{1.1}$ is capable of releasing partially from the phospholipid surface while interacting with E_4. Additionally,

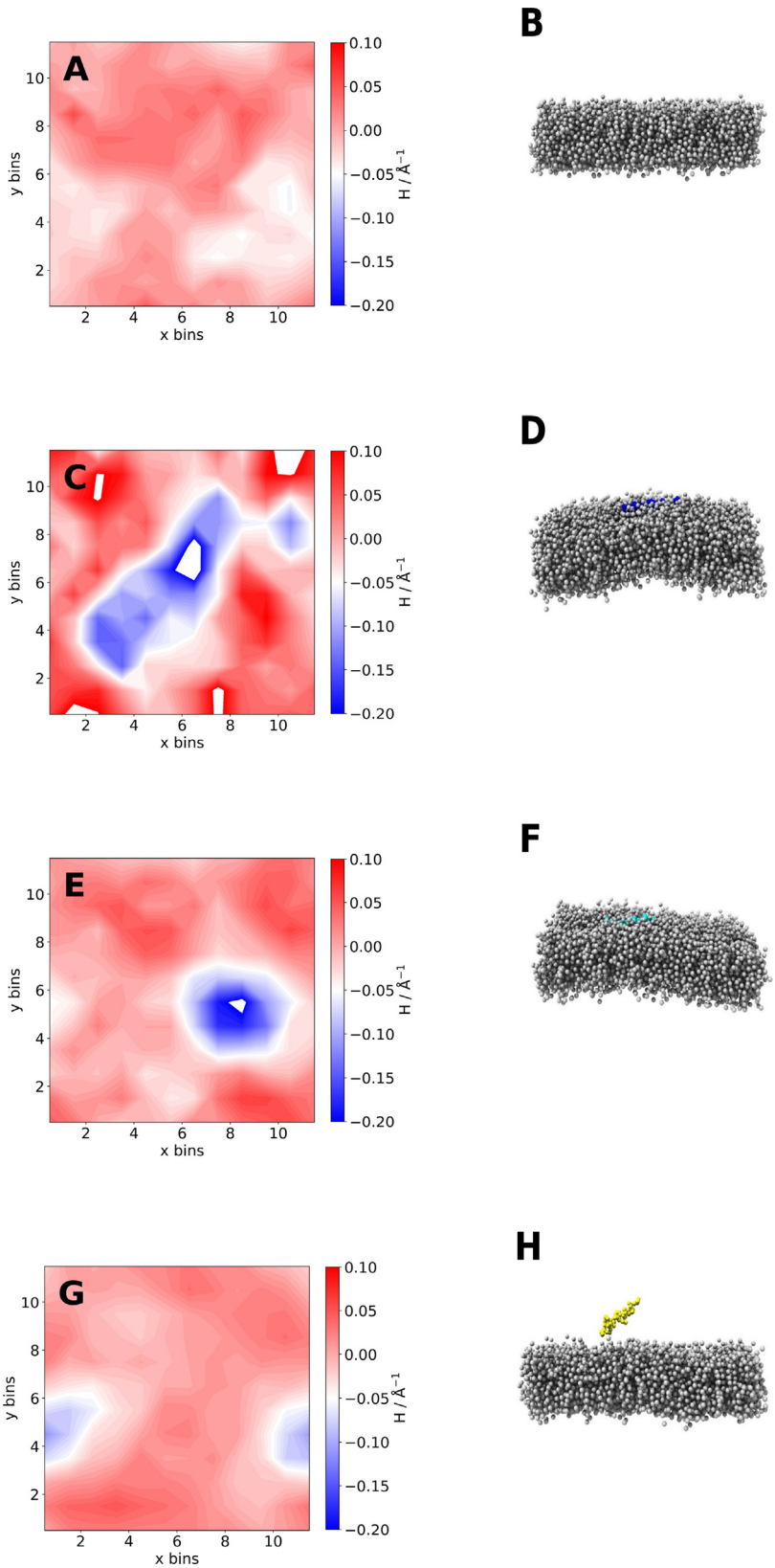

Fig. 5. Mean curvature of A: membrane without peptide, membrane with C: R_4, E: $R_{1.1}$ and G: $R_{1.4}$. (B, D, F, H): arbitrary chosen snapshots of system A, C, D and E respectively.

what is interesting from $R_{1.1}$–E_4–membrane interaction, is that the CC complex between $R_{1.1}$–E_4 is no longer shifted comparing to CC in the absence of membrane, and is closer to the expected parallel CC structure. This could be due to the fact of ARG1 moiety interacting with lipid membrane and not available for binding to two glutamic acid residues. Finally, $R_{1.4}$ does not form hydrogen bond with the membrane and there is only 1 hydrogen bond between $R_{1.4}$ and

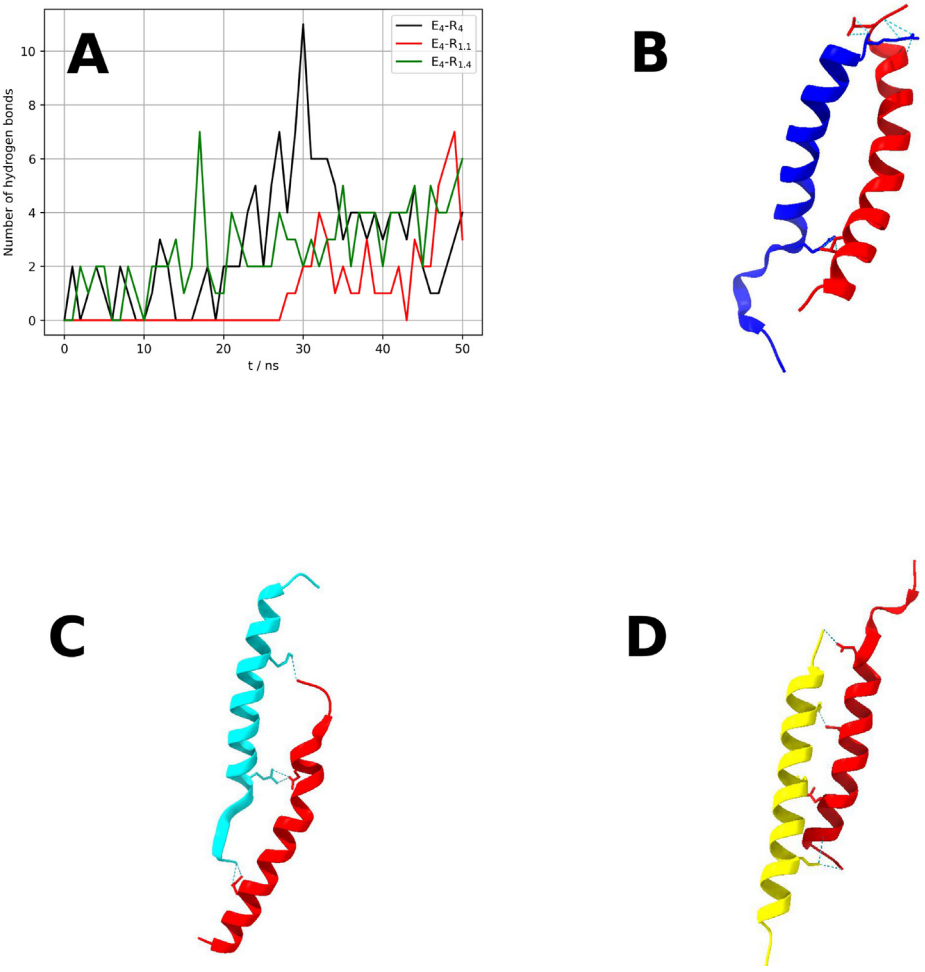

Fig. 6. A: Number of hydrogen bonds of R_4, $R_{1.1}$, $R_{1.4}$ with E_4. Hydrogen bonds between B: R_4 and E_4, C: $R_{1.1}$ and E_4 and D: $R_{1.4}$ and E_4.

Table 2
Hydrogen bonds between R_4 and E_4 and $R_{1.1}$ and E_4.

R_4 – E_4	$R_{1.1}$ – E_4	$R_{1.4}$ – E_4
ARG1–GLU27	ARG1–GLU8	LYS1–GLU8
ARG1–ALA24	ARG1–GLU15	LYS6–GLU15
ARG20–GLU8	ARG6–GLU22	LYS13–GLU22
ARG22–LEU19	ARG6–GLU22	LYS20–ALA24
ARG22–GLU21	ARG6–GLU22	LYS20–LYS28

E_4 after the simulation which cannot be considered as a significant manifestation of interaction.

Since the peptides can only be suitable fusogen if persists their capability of forming coiled-coil complex when bound to the membrane, we can conclude that $R_{1.4}$ is not suitable as fusogen but in the same time R_4 and $R_{1.1}$ are potential candidates for further experimental investigations. R_4 bonds on the surface of the membrane in an irreversible manner but still capable of forming coiled-coil complex with the partner E_4 peptide. $R_{1.1}$ has less strong binding affinity to the membrane due to the fewer arginines in its sequence, but the peptide–membrane interaction is sustained upon forming coiled-coil complex with E_4.

4. Conclusion

The understanding of interaction of SNARE peptides with phospholipid membranes is crucial in order to better understand the indication of membrane fusion processes. To understand the effect of insertion of dehydrating amino acids into the SNARE peptide sequence, we investigated the binding affinity of arginine modified K peptides to be used as fusogens with all-atomic and coarse-grained molecular dynamics simulation. We found that introducing arginine into SNARE peptide sequences can enhance the binding affinity to the membrane via hydrogen bonds and the incorporation of arginine residues into the N–terminal position is influential in binding to the surface of the membrane. Beside binding to the membrane, arginine modified SNARE peptides are capable of forming coiled-coil complex with the appropriate partner peptide which is an important step in the fusion mechanism.

In summary, arginine modified SNARE peptides are potentially applicable for further *in silico and experimental investigations, enhancing the detailed understanding of fusion processes. Therefore, in future studies, we will conduct further simulations with more emphasis on lipid clustering caused by the peptide and we will be synthesizing and exploring fusion assays of a library of peptides with arginines incorporated in their sequence and validate the peptide–membrane interactions predicted in the simulations by scattering and microscopic techniques.*

Declaration of Competing Interest

The authors declare that they have no known competing financial interests or personal relationships that could have appeared to influence the work reported in this paper.

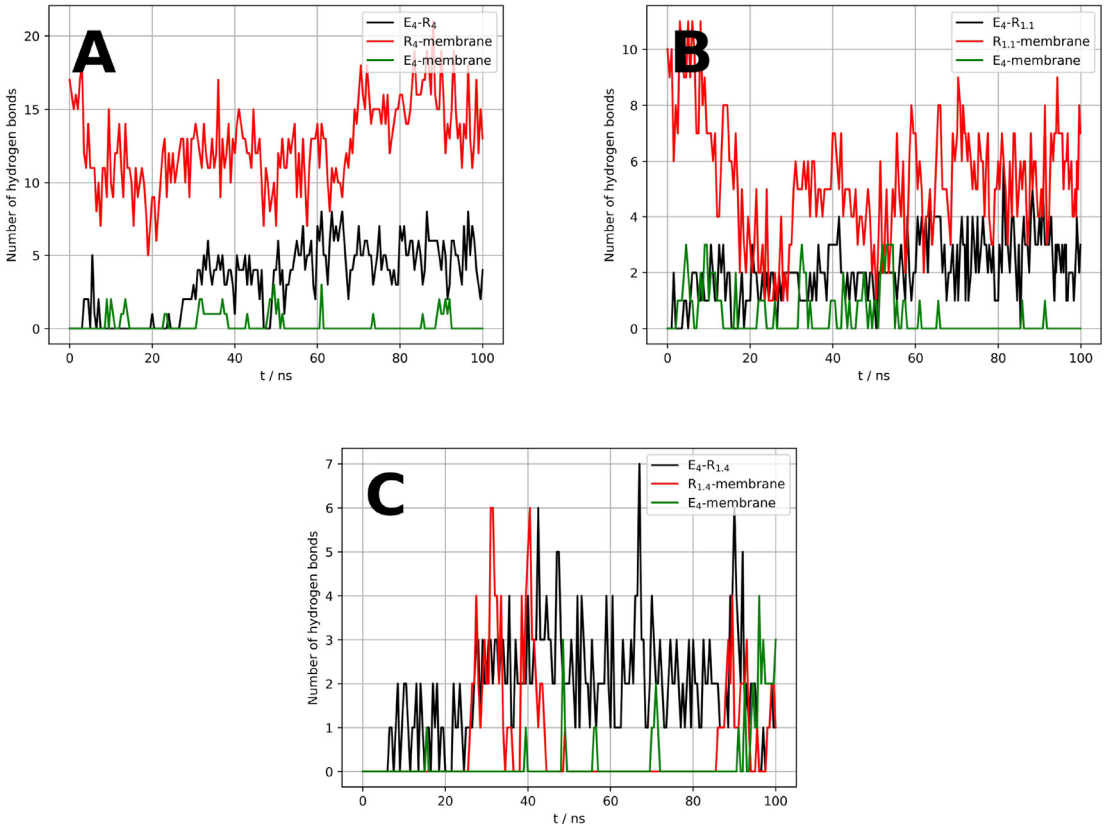

Fig. 7. Number of hydrogen bonds between peptide–peptide and peptides–membrane for A: R_4–E_4–membrane, B: $R_{1.1}$–E_4–membrane and C: $R_{1.4}$–E_4–membrane system.

Table 3
Hydrogen bond lifetime of all systems.

System name	Hydrogen bond lifetime/ ps
R_4–membrane	9.143
$R_{1.1}$–membrane	2.246
$R_{1.4}$–membrane	3.063
R_4–E_4	2.526
$R_{1.1}$–E_4	2.812
$R_{1.4}$–E_4	7.310
R_4–E_4 in R_4–E_4–membrane	10.361
R_4–membrane in R_4–E_4–membrane	7.573
E_4–membrane in R_4–E_4–membrane	2.892
$R_{1.1}$–E_4 in $R_{1.1}$–E_4–membrane	11.572
$R_{1.1}$–membrane in $R_{1.1}$–E_4–membrane	6.501
E_4–membrane in $R_{1.1}$–E_4–membrane	2.280
$R_{1.4}$–E_4 in $R_{1.4}$–E_4–membrane	4.745
$R_{1.4}$–membrane in $R_{1.4}$–E_4–membrane	2.005
E_4–membrane in $R_{1.4}$–E_4–membrane	1.703

Acknowledgments

The authors acknowledge the Dutch Ministry of Education, Culture and Science (Gravity Program 024.001.035) for financial support and [KIFÜ] for awarding us access to resources based in Hungary at Debrecen for CPU time.

Appendix A. Supplementary material

Supplementary data associated with this article can be found, in the online version, at https://doi.org/10.1016/j.molliq.2022.119972.

References

[1] B.C. Buddingh, J.C.M.v. Hest, Engineering interactive artificial cells Ph.D. thesis, Technische Universiteit Eindhoven, Eindhoven, 2020.
[2] E. Sackmann, Structure and Dynamics of Membranes, Handbook of Biological Physics 1 (1995), https://doi.org/10.1016/S1383-8121(06)80018-7.
[3] C. Du, C. Webb, Cellular Systems, Engineering Fundamentals of Biotechnology, 11–23, Elsevier BV, 2011, https://doi.org/10.1016/B978-0-08-088504-9.00080-5.
[4] H. Robson Marsden, I. Tomatsu, A. Kros, Model systems for membrane fusion, Chemical Society Reviews 40 (3) (2011) 1572–1585, publisher: Royal Society of Chemistry. doi:10.1039/C0CS00115E.
[5] S.E. Diltemiz, M. Tavafoghi, N.R. d. Barros, M. Kanada, J. Heinämäki, C. Contag, S. K. Seidlits, N. Ashammakhi, Use of artificial cells as drug carriers, Materials Chemistry Frontiers 5 (18) (2021) 6672–6692, publisher: Royal Society of Chemistry. doi:10.1039/D1QM00717C.
[6] Y. Yano, A. Yano, S. Oishi, Y. Sugimoto, G. Tsujimoto, N. Fujii, K. Matsuzaki, Coiled-coil tag - Probe system for quick labeling of membrane receptors in living cells, ACS Chem. Biol. 3 (6) (2008) 341–345, https://doi.org/10.1021/cb8000556.
[7] H.R. Marsden, A.V. Korobko, T. Zheng, J. Voskuhl, A. Kros, Controlled liposome fusion mediated by SNARE protein mimics, Biomaterials Science 1 (10) (2013) 1046–1054, https://doi.org/10.1039/c3bm60040h.
[8] G.A. Daudey, M. Shen, A. Singhal, P. van der Est, G.J. Sevink, A.L. Boyle, A. Kros, Liposome fusion with orthogonal coiled coil peptides as fusogens: The efficacy of roleplaying peptides, Chemical Science 12 (41) (2021) 13782–13792, https://doi.org/10.1039/d0sc06635d.
[9] H.R. Marsden, N.A. Elbers, P.H. Bomans, N.A. Sommerdijk, A. Kros, A Reduced SNARE model for membrane fusion, Angewandte Chemie - International Edition 48 (13) (2009) 2330–2333, https://doi.org/10.1002/anie.200804493.
[10] J.R. Litowski, R.S. Hodges, Designing heterodimeric two-stranded α-helical coiled-coils. Effects of hydrophobicity and α-helical propensity on protein folding, stability, and specificity, Journal of Biological Chemistry 277 (40) (2002) 37272–37279. doi:10.1074/jbc.M204257200.
[11] A.W. Reinke, R.A. Grant, A.E. Keating, A synthetic coiled-coil interactome provides heterospecific modules for molecular engineering, J. Am. Chem. Soc. 132 (17) (2010) 6025–6031, https://doi.org/10.1021/ja907617a.
[12] E.H. Bromley, R.B. Sessions, A.R. Thomson, D.N. Woolfson, Designed α-helical tectons for constructing multicomponent synthetic biological systems, J. Am. Chem. Soc. 131 (3) (2009) 928–930, https://doi.org/10.1021/ja804231a.
[13] J.M. Fletcher, A.L. Boyle, M. Bruning, S.J. Bartlett, T.L. Vincent, N.R. Zaccai, C.T. Armstrong, E.H. Bromley, P.J. Booth, R.L. Brady, A.R. Thomson, D.N. Woolfson, A

basis set of de novo coiled-Coil peptide oligomers for rational protein design and synthetic biology, ACS Synthetic Biology 1 (6) (2012) 240–250, https://doi.org/10.1021/sb300028q.
[14] C. Aronsson, S. Dånmark, F. Zhou, P. Öberg, K. Enander, H. Su, D. Aili, Self-sorting heterodimeric coiled coil peptides with defined and tuneable self-assembly properties, Scientific Reports 5 (2015) 1–10, https://doi.org/10.1038/srep14063.
[15] P. Burkhard, J. Stetefeld, S.V. Strelkov, Coiled coils: A highly versatile protein folding motif, Trends Cell Biol. 11 (2) (2001) 82–88, https://doi.org/10.1016/S0962-8924(00)01898-5.
[16] S. Marqusee, R.L. Baldwin, Helix stabilization by Glu-...Lys+ salt bridges in short peptides of de novo design., Proceedings of the National Academy of Sciences of the United States of America 84 (24) (1987) 8898–8902. doi:10.1073/pnas.84.24.8898.
[17] N.E. Zhou, C.M. Kay, R.S. Hodges, The role of interhelical ionic interactions in controlling protein folding and stability: De novo designed synthetic two-stranded α-helical coiled-coils (1994). doi:10.1006/jmbi.1994.1250.
[18] E.K. O'Shea, K.J. Lumb, P.S. Kim, Peptide 'Velcro': Design of a heterodimeric coiled coil, Curr. Biol. 3 (10) (1993) 658–667, https://doi.org/10.1016/0960-9822(93)90063-T.
[19] N.L. Mora, A.L. Boyle, B.J. van Kolck, A. Rossen, Š. Pokorná, A. Koukalová, R. Šachl, M. Hof, A. Kros, Controlled Peptide-Mediated Vesicle Fusion Assessed by Simultaneous Dual-Colour Time-Lapsed Fluorescence Microscopy, Scientific Reports 10 (1) (2020) 1–13, https://doi.org/10.1038/s41598-020-59926-z.
[20] T. Zheng, J. Voskuhl, F. Versluis, H.R. Zope, I. Tomatsu, H. Robson Marsden, A. Kros, Controlling the rate of coiled coil driven membrane fusion, Chemical Communications 49 (35) (2013) 3649–3651. doi:10.1039/c3cc38926j.
[21] H.R. Marsden, A.V. Korobko, T. Zheng, J. Voskuhl, A. Kros, Controlled liposome fusion mediated by SNARE protein mimics, Biomaterials Science 1 (10) (2013) 1046–1054, publisher: Royal Society of Chemistry. doi:10.1039/C3BM60040H.
[22] M. Rabe, H.R. Zope, A. Kros, Interplay between Lipid Interaction and Homo-coiling of Membrane-Tethered Coiled-Coil Peptides, Langmuir 31 (36) (2015) 9953–9964, publisher: American Chemical Society. doi:10.1021/acs.langmuir.5b02094.
[23] M. Rabe, C. Schwieger, H.R. Zope, F. Versluis, A. Kros, Membrane Interactions of Fusogenic Coiled-Coil Peptides: Implications for Lipopeptide Mediated Vesicle Fusion, Langmuir 30 (26) (2014) 7724–7735, publisher: American Chemical Society. doi:10.1021/la500987c.
[24] M. Rabe, C. Aisenbrey, K. Pluhackova, V. de Wert, A.L. Boyle, D.F. Bruggeman, S. A. Kirsch, R.A. Böckmann, A. Kros, J. Raap, B. Bechinger, A Coiled-Coil Peptide Shaping Lipid Bilayers upon Fusion, Biophys. J . 111 (10) (2016) 2162–2175, https://doi.org/10.1016/j.bpj.2016.10.010.
[25] M. Bulacu, G.J.A. Sevink, Computational insight in the role of fusogenic lipopeptides at the onset of liposome fusion, Biochimica et Biophysica Acta (BBA) -, Biomembranes 1848 (8) (2015) 1716–1725, https://doi.org/10.1016/j.bbamem.2015.03.016.
[26] K. Pluhackova, T.A. Wassenaar, S. Kirsch, R.A. Böckmann, Spontaneous Adsorption of Coiled-Coil Model Peptides K and E to a Mixed Lipid Bilayer, The Journal of Physical Chemistry B 119 (12) (2015) 4396–4408, publisher: American Chemical Society. doi:10.1021/acs.jpcb.5b00434.
[27] G.A. Daudey, C. Schwieger, M. Rabe, A. Kros, Influence of Membrane-Fusogen Distance on the Secondary Structure of Fusogenic Coiled Coil Peptides, Langmuir (2019), https://doi.org/10.1021/acs.langmuir.8b04195.
[28] F. Versluis, J. Voskuhl, B. Van Kolck, H. Zope, M. Bremmer, T. Albregtse, A. Kros, In situ modification of plain liposomes with lipidated coiled coil forming peptides induces membrane fusion, J. Am. Chem. Soc. 135 (21) (2013) 8057–8062, https://doi.org/10.1021/ja4031227.
[29] N. Kanwa, S.K. De, A. Maity, A. Chakraborty, Interaction of aliphatic amino acids with zwitterionic and charged lipid membranes: Hydration and dehydration phenomena, PCCP 22 (6) (2020) 3234–3244, https://doi.org/10.1039/c9cp06188f.
[30] L. Li, I. Vorobyov, T.W. Allen, The different interactions of lysine and arginine side chains with lipid membranes, J. Phys. Chem. B 117 (40) (2013) 11906–11920, https://doi.org/10.1021/jp405418y.
[31] M. Vazdar, J. Heyda, P.E. Mason, G. Tesei, C. Allolio, M. Lund, P. Jungwirth, Arginine magic: Guanidinium Like-Charge Ion Pairing from Aqueous Salts to Cell Penetrating Peptides, Acc. Chem. Res. 51 (6) (2018) 1455–1464, https://doi.org/10.1021/acs.accounts.8b00098.
[32] S. Pronk, S. Páll, R. Schulz, P. Larsson, P. Bjelkmar, R. Apostolov, M.R. Shirts, J.C. Smith, P.M. Kasson, D. van der Spoel, B. Hess, E. Lindahl, GROMACS 4.5: a high-throughput and highly parallel open source molecular simulation toolkit, Bioinformatics 29 (7) (2013) 845–854. doi:10.1093/bioinformatics/btt055.
[33] M.J. Abraham, T. Murtola, R. Schulz, S. Páll, J.C. Smith, B. Hess, E. Lindahl, GROMACS: High performance molecular simulations through multi-level parallelism from laptops to supercomputers, SoftwareX 1–2 (2015) 19–25, https://doi.org/10.1016/j.softx.2015.06.001.
[34] A. Lamiable, P. Thévenet, J. Rey, M. Vavrusa, P. Derreumaux, P. Tufféry, PEP-FOLD3: faster de novo structure prediction for linear peptides in solution and in complex, Nucleic Acids Res. 44 (W1) (2016) W449–W454, https://doi.org/10.1093/nar/gkw329.
[35] Y. Shen, J. Maupetit, P. Derreumaux, P. Tufféry, Improved PEP-FOLD Approach for Peptide and Miniprotein Structure Prediction, Journal of Chemical Theory and Computation 10 (10) (2014) 4745–4758, publisher: American Chemical Society. doi:10.1021/ct500592m.
[36] P. Thévenet, Y. Shen, J. Maupetit, F. Guyon, P. Derreumaux, P. Tufféry, PEP-FOLD: an updated de novo structure prediction server for both linear and disulfide bonded cyclic peptides, Nucleic Acids Res. 40 (W1) (2012) W288–W293, https://doi.org/10.1093/nar/gks419.
[37] S. Jo, J.B. Lim, J.B. Klauda, W. Im, CHARMM-GUI Membrane Builder for Mixed Bilayers and Its Application to Yeast Membranes, Biophys. J . 97 (1) (2009) 50–58, https://doi.org/10.1016/j.bpj.2009.04.013.
[38] J. Lee, X. Cheng, J.M. Swails, M.S. Yeom, P.K. Eastman, J.A. Lemkul, S. Wei, J. Buckner, J.C. Jeong, Y. Qi, S. Jo, V.S. Pande, D.A. Case, C.L. Brooks, A.D. MacKerell, J.B. Klauda, W. Im, CHARMM-GUI Input Generator for NAMD, GROMACS, AMBER, OpenMM, and CHARMM/OpenMM Simulations Using the CHARMM36 Additive Force Field, Journal of Chemical Theory and Computation 12 (1) (2016) 405–413, publisher: American Chemical Society. doi:10.1021/acs.jctc.5b00935.
[39] R.B. Best, X. Zhu, J. Shim, P.E.M. Lopes, J. Mittal, M. Feig, A.D. MacKerell, Optimization of the Additive CHARMM All-Atom Protein Force Field Targeting Improved Sampling of the Backbone ϕ, $\psi$and Side-Chain χ1 and χ2 Dihedral Angles, Journal of Chemical Theory and Computation 8 (9) (2012) 3257–3273, publisher: American Chemical Society. doi:10.1021/ct300400x.
[40] J.B. Klauda, R.M. Venable, J.A. Freites, J.W. O'Connor, D.J. Tobias, C. Mondragon-Ramirez, I. Vorobyov, A.D. MacKerell, R.W. Pastor, Update of the CHARMM All-Atom Additive Force Field for Lipids: Validation on Six Lipid Types, The Journal of Physical Chemistry B 114 (23) (2010) 7830–7843, publisher: American Chemical Society. doi:10.1021/jp101759q.
[41] J. Chen, F. Dai, L. Zhang, J. Xu, W. Liu, S. Zeng, C. Xu, L. Chen, C. Dai, Molecular insights into the dispersion stability of graphene oxide in mixed solvents: Theoretical simulations and experimental verification, J. Colloid Interface Sci. 571 (2020) 109–117, https://doi.org/10.1016/j.jcis.2020.03.036.
[42] S. Akbarzadeh, M. Ramezanzadeh, B. Ramezanzadeh, G. Bahlakeh, A green assisted route for the fabrication of a high-efficiency self-healing anti-corrosion coating through graphene oxide nanoplatform reduction by Tamarindus indiaca extract, J. Hazard. Mater. 390 (2020) 122147, https://doi.org/10.1016/j.jhazmat.2020.122147.
[43] S. Nosé, M. Klein, Constant pressure molecular dynamics for molecular systems, Molecular Physics 50 (5) (1983) 1055–1076, publisher: Taylor & Francis _eprint: doi: 10.1080/00268978300102851. doi:10.1080/00268978300102851.
[44] S. Nosé, A molecular dynamics method for simulations in the canonical ensemble, Molecular Physics 52 (2) (1984) 255–268, publisher: Taylor & Francis _eprint: doi: 10.1080/00268978400101201. doi:10.1080/00268978400101201.
[45] W.G. Hoover, Canonical dynamics: Equilibrium phase-space distributions, Physical Review A 31 (3) (1985) 1695–1697, publisher: American Physical Society. doi:10.1103/PhysRevA.31.1695.
[46] M. Parrinello, A. Rahman, Polymorphic transitions in single crystals: A new molecular dynamics method, Journal of Applied Physics 52 (12) (1981) 7182–7190, publisher: American Institute of Physics. doi:10.1063/1.328693.
[47] B. Hess, H. Bekker, H.J.C. Berendsen, J.G.E.M. Fraaije, LINCS: A linear constraint solver for molecular simulations, J. Comput. Chem. 18 (12) (1997) 1463–1472, https://doi.org/10.1002/(SICI)1096-987X(199709)18:12<1463::AID-JCC4>3.0.CO;2-H.
[48] D.H. de Jong, G. Singh, W.F.D. Bennett, C. Arnarez, T.A. Wassenaar, L.V. Schäfer, X. Periole, D.P. Tieleman, S.J. Marrink, Improved Parameters for the Martini Coarse-Grained Protein Force Field, Journal of Chemical Theory and Computation 9 (1) (2013) 687–697, publisher: American Chemical Society. doi:10.1021/ct300646g.
[49] S.O. Yesylevskyy, L.V. Schäfer, D. Sengupta, S.J. Marrink, Polarizable Water Model for the Coarse-Grained MARTINI Force Field, PLOS Computational Biology 6 (6) (2010) e1000810, publisher: Public Library of Science. doi:10.1371/journal.pcbi.1000810.
[50] G. Bussi, D. Donadio, M. Parrinello, Canonical sampling through velocity rescaling, The Journal of Chemical Physics 126 (1) (2007) 014101, publisher: American Institute of Physics. doi:10.1063/1.2408420.
[51] E.F. Pettersen, T.D. Goddard, C.C. Huang, G.S. Couch, D.M. Greenblatt, E.C. Meng, T.E. Ferrin, UCSF Chimera—A visualization system for exploratory research and analysis, Journal of Computational Chemistry 25 (13) (2004) 1605–1612, _eprint: https://onlinelibrary.wiley.com/doi/pdf/10.1002/jcc.20084. doi:10.1002/jcc.20084.
[52] N. Michaud-Agrawal, E.J. Denning, T.B. Woolf, O. Beckstein, Mdanalysis: a toolkit for the analysis of molecular dynamics simulations, Journal of computational chemistry 32 (10) (2011) 2319–2327.
[53] R.J. Gowers, M. Linke, J. Barnoud, T.J. Reddy, M.N. Melo, S.L. Seyler, J. Domanski, D.L. Dotson, S. Buchoux, I.M. Kenney, et al., Mdanalysis: a python package for the rapid analysis of molecular dynamics simulations, in: Proceedings of the 15th python in science conference, Vol. 98, SciPy Austin, TX, 2016, p. 105.
[54] S. Woo, H. Lee, All-atom simulations and free-energy calculations of coiled-coil peptides with lipid bilayers: Binding strength, structural transition, and effect on lipid dynamics, Scientific Reports 6 (2016), https://doi.org/10.1038/srep22299.
[55] D. van der Spoel, P.J. van Maaren, P. Larsson, N. Tımneanu, Thermodynamics of hydrogen bonding in hydrophilic and hydrophobic media, J. Phys. Chem. B 110 (9) (2006) 4393–4398.
[56] M. Abraham, D. Van Der Spoel, E. Lindahl, B. Hess, et al., Gromacs user manual version, 5.0. 4, Royal Institute of Technology and Uppsala University, Sweden, 2014.
[57] D.P. Tieleman, S.-J. Marrink, H.J. Berendsen, A computer perspective of membranes: molecular dynamics studies of lipid bilayer systems. doi:10.1016/S0304-4157(97)00008-7.

[58] Y. Song, V. Guallar, N.A. Baker, Molecular Dynamics Simulations of Salicylate Effects on the Micro- and Mesoscopic Properties of a Dipalmitoylphosphatidylcholine Bilayer, Biochemistry 44 (41) (2005) 13425–13438, publisher: American Chemical Society. doi:10.1021/bi0506829.
[59] T.J. Piggot, J.R. Allison, R.B. Sessions, J.W. Essex, On the Calculation of Acyl Chain Order Parameters from Lipid Simulations, Journal of Chemical Theory and Computation 13 (11) (2017) 5683–5696, publisher: American Chemical Society. doi:10.1021/acs.jctc.7b00643.
[60] Z. Chen, Y. Mao, J. Yang, T. Zhang, L. Zhao, K. Yu, M. Zheng, H. Jiang, H. Yang, Characterizing the binding of annexin V to a lipid bilayer using molecular dynamics simulations, Proteins: Structure, Function, and Bioinformatics 82 (2) (2014) 312–322, _eprint: https://onlinelibrary.wiley.com/doi/pdf/10.1002/prot.24389. doi:10.1002/prot.24389.